Title:

A non-coding plant pathogen provokes both transcriptional and posttranscriptional alterations in tomato

Authors:

Purificación Lisón*[1], Susana Tárraga*[1], Mª Pilar López-Gresa[1], Asunción Saurí[1], Cristina Torres[1], Laura Campos[1], José Mª Bellés[1], Vicente Conejero[1] and Ismael Rodrigo[1]**

[1]Instituto de Biología Molecular y Celular de Plantas. Universitat Politècnica de València (UPV) - Consejo Superior de Investigaciones Científicas (CSIC).

* These authors contributed equally to this work.

**Corresponding author

Dr. Ismael Rodrigo e-mail: irodrig@ibmcp.upv.es

Phone: +34 96 3877862, Fax: +34 96 3877859,

Instituto de Biología Molecular y Celular de Plantas. Universitat Politècnica de València (UPV) - Consejo Superior de Investigaciones Científicas (CSIC).

CPI - Edif. 8E

Ingeniero Fausto Elío S/N

46022 - Valencia

SPAIN

Abbreviations

BP	Band-Pass
BVA	Biological Variation Analysis
CEVd	*Citrus exocortis viroid*
DIA	Differential In-gel Analysis
eEF1A	eukaryotic Elongation Factor 1
eEF2	eukaryotic Elongation Factor 2
eIF5A	eukaryotic translation Initiation Factor 5-Alpha
FDR	False Discovery Rate
GA	Gentisic Acid
PRs	Pathogenesis-Related proteins
PSTVd	Potato Spindle Tuber Viroid
PVP	Polyvinylpyrrolidone
SA	Salicylic Acid

Keywords

Tomato/Viroid/2-D-DIGE/Plant stress/Translation factors

Total number of words

7253

Abstract

Viroids are single-stranded, circular, non-coding RNAs that infect plants, causing devastating diseases. In this work, we employed two-dimensional DIGE, followed by mass spectrometry identification, to analyze the response of tomato plants infected by *Citrus exocortis viroid* (CEVd). Among the differentially expressed proteins detected, 45 were successfully identified and classified into different functional categories. Validation results by RT-PCR allowed us to classify the proteins into two expression groups. First group included genes with changes at the transcriptional level upon CEVd infection, such as an endochitinase, a β-glucanase and pathogenesis-related proteins PR10 and P69G. All these defence proteins were also induced by gentisic acid, a pathogen-induced signal in compatible interactions. The second group of proteins showed no changes at the transcriptional level and included several ribosomal proteins and translation factors, such as the elongation factors 1 and 2 and the translation initiation factor 5-alpha. These results were validated by 2-D-Western blot, and possible posttranslational modifications caused by CEVd infection were detected. Moreover, an interaction between eEF1A and CEVd was observed by 2-D-Northwestern. The present study provides new protein-related information on the mechanisms of plant resistance to pathogens.

1. Introduction

Viroids consist of a naked, covalently closed, single-stranded RNA of small size (250-400 nucleotides) that does not contain any open reading frame [1, 2]. Even without encoding any protein to provide specific functions, viroids are able to replicate in host cells and spread through the plant vascular system to establish a systemic infection, causing very severe diseases, even death [3-5]. These circular RNAs can further enlist host-encoded factors for replicating themselves. However, except for the polymerases used for replication, the host proteins involved in viroid systemic infection remain largely unknown [6, 7].

Citrus exocortis viroid (CEVd), the causal agent of the exocortis disease of citrus plants, produces a systemic, compatible infection in tomato resulting in plant stunting, an extreme leaf epinasty and rugosity, and the *de novo* synthesis of Pathogenesis-Related (PR) proteins [8-11]. The levels of different signal molecules such as salicylic acid (SA), ethylene or polyamines are severely altered [12-14]. CEVd infection strongly induces the accumulation of gentisic acid (GA), both as a free form or conjugated to xylose in tomato plants [14-16]. GA, a metabolite derivative of SA, has been proposed as a signal molecule for plant defence response in compatible, non-necrotizing, interactions. It has been described that the accumulation of GA is higher than other signal molecules such as salicylic acid (SA), in many compatible plant-pathogen interactions. Moreover, exogenous GA elicits the induction of pathogenesis-related proteins (PRs) which are not induced by SA [14, 17]. Recently, a metabolomic study of viroid-infected tomato plants has confirmed the strong accumulation of GA in this compatible interaction [18].

Recently, a number of proteomic studies have been carried out to investigate the plant response to different pathogens [19-23]. All these proteome-based approaches have provided a better picture of the regulatory elements in plant-pathogen interactions. Unlike other pathogens, which can produce different polypeptides involved in the plant attack or the

symptom development, viroid RNA sequence does not encode for any known protein. Therefore the dramatic symptom development observed upon viroid infection is produced by the plant itself as a consequence of a severe interference of the viroid RNA in important cell processes. In this respect, proteomics constitutes a powerful tool to study the protein alterations produced by viroid infection. In our research presented in this manuscript, we applied 2-D DIGE technology coupled with mass spectrometry to carry out a proteomic analysis of the plant-viroid interaction for the first time. Differentially expressed proteins were further studied by using RT-PCR or 2-D Western blot to confirm the proteomic data. The goal was to identify proteins possibly implicated in the plant defence response and the involvement of GA in the induction of these proteins. Additionally, post-translational modifications provoked by viroid infection and possible protein-viroid interactions have been studied.

2. Materials and methods

2.1. Plant material, viroid inoculation and treatments

Tomato plants (*Solanum lycopersicum* L. cv Rutgers) were grown (one per pot) in a phytochamber at 30 °C for 16 h with fluorescent light and at 25 °C for 8 h in darkness. Inoculation of plants with *Citrus exocortis viroid* (CEVd) was carried out by puncturing the stems of the seedlings with a needle dipped in either buffer or the nucleic acid preparation according to Granell *et al.* [8] and Bellés *et al.* [24]. Leaf tissue was collected 20 days after viroid inoculation Treatments with gentisic acid (GA) or salicylic acid (SA) were performed using fully expanded leaves from one-month old plants. Leaves were excised and petioles were immersed in 10 mM phosphate (pH 7.4) buffer solutions containing 2 mM GA or 0.5 mM SA. We have previously observed that these concentrations induce resistance to RNA pathogens in tomato (our unpublished data)

Leaf material was harvested at different time points (0, 1, 4, 8 and 24 hours after treatment), put in liquid nitrogen and stored frozen at -80 ºC.

2.2. Protein extraction

Frozen tomato leaves were reduced to dust with liquid nitrogen using mortar and pestle in the presence of 0.05% (w/w) PVP. Then, extraction buffer (50 mM Tris-HCl, pH 7.5, 1 mM PMSF, 0.2% β-mercaptoethanol) was added (2 mL/gram fresh weight), and plant material was homogenized. The crude mixtures were centrifuged for 20 min at 20.000 *g*. Supernatants were mixed with an equal volume of cold 20% TCA, incubated for 1 h at 4 ºC and centrifuged at 20.000 *g* for 15 min at 4 ºC. The protein pellets were washed three times with acetone. Pellets were then dissolved in lysis buffer (7 M urea, 2 M thiourea, 4% CHAPS). Protein aliquots to be analyzed by 2-D electrophoresis were stripped of non-protein contaminants using a 2-D Clean-Up Kit (GE Healthcare). The resulting proteins were dissolved in lysis buffer for conventional 2-D analysis or in a Tris-buffered solution (7 M urea, 2 M thiourea, 4% CHAPS, 20 mM Tris-HCl, pH 8.5) for 2-D DIGE analysis. Protein concentration was determined with the Sigma Bradford Reagent using bovine serum albumin (BSA) as standard.

2.3. Gel imaging and data analysis

The scanned pictures were then directly transferred to the ImageQuant V5.2 software package (GE Healthcare). Image gel analysis was carried out using the DeCyder 2D Software V6.5 (GE Healthcare). The images were exported to the DeCyder Batch Processor module, and DIA (Differential In-gel Analysis) and BVA (Biological Variation Analysis) modules were run in automatic mode. DIA module was used for spot detection, spot volume quantification and volume ratio normalization of different samples in the same gel. BVA

module was used to match protein spots among different gels and to identify protein spots that exhibited significant differences. Manual editing was performed in the biological variation analysis module to ensure that spots were correctly matched between different gels and were not contaminated with artefacts, such as streaks or dust. The paired *t*-test was used for statistical analysis of the data. We have considered as "paired samples" those belonging to the same batch, corresponding to plants grown at the same time and in the same conditions.

To eliminate false positives, a false discovery rate (FDR) correction was routinely applied to all spots assigned as valid proteins using the DeCyder's default parameters.

Protein spots that showed a statistically significant change in abundance between control and infected material using a Student´s *t*-test ($p < 0.05$) were considered as being differentially expressed in response to the CEVd infection.

2.4. In-gel tryptic digestion, mass spectrometry and database searching

Protein identification was performed by the Proteomic Service of the CIFP (Centro de Investigación Príncipe Felipe, Valencia, Spain), which is a member of ProteoRed (http://www.proteored.org).

For picking spots of interest, CyDye gels were stained using the Protein Silver Staining Kit (GE Healthcare). Proteins were excised using an Ettan Spot Picker (GE Healthcare), and destained with two 5-min washes with ACN/H_2O (1:1, v/v), followed by rehydration with 50 mM ammonium bicarbonate for 5 min and 25 mM ammonium bicarbonate in 50% (v/v) ACN for 15 min. Gel pieces were then manually digested with sequencing grade trypsin (Promega) as described elsewhere [25], and subjected to MALDI MS/MS and/or LC/MS/MS analyses (see Supporting Information).

The samples were analyzed using the 4700 Proteomics Analyzer (Applied Biosystems, Foster City, USA) in positive reflector mode (2000 shots per spot). Five of the most intense

precursors (according to the threshold criteria: minimum signal-to-noise: 10; minimum cluster area: 500; maximum precursor gap: 200 ppm; maximum fraction gap: 4) were selected for every spot for the MS/MS analysis. MS/MS data was acquired using the manufacturer default 1 kV MS/MS method. Database searches on Swiss-Prot, NCBI and EST_solanum were performed using the MASCOT search engine (Matrix Science). The MS and MS/MS information was sent to MASCOT via GPS software (Applied Biosystems). Searches were done with tryptic specificity allowing one missed cleavage and a tolerance on the mass measurement of 100 ppm in MS mode and 0.6 Da for MS/MS ions. Carbamidomethylation of Cys was used as a fixed modification and oxidation of Met and deamidation of Asn and Gln as variable modifications. The samples without a positive identification were analyzed by LC/MS/MS. Peptide separation and identification by LC-MS/MS was performed using an Ultimate nano-LC system (LC Packings) and a QSTAR XL Q-TOF hybrid mass spectrometer (AB Sciex). Samples (5 µL) were delivered to the system using a FAMOS autosampler (LC Packings) at 30 µL/min, and the peptides were trapped onto a PepMap C18 pre-column (5 mm, 300 mm i.d.; LC Packings). Peptides were then eluted onto the PepMap C18 analytical column (15 cm 75 mm i.d.; LC Packings) at 300 nL/min and separated using a 30 min gradient of 5–45% ACN. The QSTAR XL was operated in information-dependent acquisition mode, in which a 1 s TOF MS scan from 400–2000 m/z, was performed, followed by 3 s product ion scans from 65–2000 m/z on the three most intense doubly or triply charged ions. The MS/MS information was sent to MASCOT via the MASCOT DAEMON ST 066 software (MATRIX SCIENCE). The search parameters were defined as for MS-MS/MS analysis above. The databases used were SwissProt 20090603, SwissProt 20100224, NCBInr 20090602, NCBInr 20100223, NCBInr 20090522 and EST_solanum solanum_210508. An extended table providing all information used for protein identification can be found in Supporting Information (Table S1).

2.5. RNA analysis

Total RNA was extracted from tomato leaf tissue ground in liquid nitrogen using the TRIzol reagent (Invitrogen). First strand cDNA was synthesized from 5 μg of total RNA obtained from different tomato tissues using Moloney murine leukemia virus reverse transcriptase (Promega) and an oligo$(dT)_{18}$ primer. Five microliters of the reverse transcriptase reaction were used for PCR, employing a Perkin-Elmer thermocycler under the following conditions: 25 or 30 cycles of 94 ºC for 30 s, 50 ºC for 1 min, and 72 ºC for 1 min, followed by a final extension of 72 ºC for 15 min. The primers used for each gene are listed in Table S2 of Supporting Information. The reference genes induced by GA and SA correspond to the tomato pathogenesis-related proteins P14 (PR1) and P23 (PR5). These two genes were used as markers for the induction of defence proteins along the viroid infection. All PCR products were detected via electrophoresis on 1% agarose gel.

2.6. Immunoblotting

Proteins separated in 2-D electrophoresis gels were transferred onto nitrocellulose membranes (24 x 20 cm) using a Hoefer SemiPhor (Pharmacia Biotech) semi-dry electrotransfer equipment.

Immuno-detection was performed using a 1:10.000 dilution of maize eEF1A antiserum, a 1:2.500 dilution of maize eEF2 antiserum (both antisera kindly provided by Dr. Brenda Hunter, University of Arizona) or a 1:5.000 dilution of *Arabidopsis* eIF5A antiserum (kindly provided by Dr. Alejandro Ferrando, Instituto de Biología Molecular y Celular de Plantas UPV-CSIC; unpublished data). Membranes were incubated with goat anti-rabbit IgG conjugated to alkaline phosphatase (Promega) as a secondary antibody. Nitroblue tetrazolium

and 5-bromo-4-chloro-3-indolyl phosphate (Sigma) were used as substrates for alkaline phosphatase following standard protocols.

2.7. 2-D Northwestern

Protein-viroid interactions were detected using radiolabelled viroid transcripts as follows. 2-D electrophoresis gels were prepared in triplicate: one gel was used for silver-staining to identify protein spots, another one was used for Western blot (see *Immunoblotting* above), and the third gel was subjected to a Northwestern hybridization as described in Dubé *et al*. [26]. Briefly, proteins from the 2-D gel were transferred onto nitrocellulose membranes, then the membranes were washed three times in 25 ml of Northwestern buffer (10 mM Tris-HCl pH 7.4, 50 mM NaCl, 1 mM EDTA, 400 g/ml Ficoll 400, 400 g/ml PVP, 400 g/ml bovine serum albumin, and fresh 1 mM DTT) for 20 min at room temperature. Then, after a preincubation of 1 h in 25 ml of Northwestern buffer which served as a renaturation step, yeast tRNA (20 g/ml) and 5.000 cpm of radioactive CEVd RNA probe were added to the buffer solution, and the hybridization was performed at room temperature for 1 h. The membranes were washed three times in Northwestern buffer for 10 min and then were revealed by autoradiography.

3. Results

3.1. Identification of differentially expressed proteins in response to CEVd infection by 2-D DIGE and mass spectrometry

Tomato seedlings were inoculated with CEVd, and 20 days after inoculation the plants presented stunting, an extreme leaf epinasty and rugosity, thus indicating that a systemic infection was clearly established. At that stage, protein profiles of both control and CEVd-

infected plants were compared by using 2-D DIGE, in order to identify proteins differentially regulated by this infection. Four biological replicates were prepared. A total of 1481 spots were located in the four gels. Quantitative comparisons of viroid-infected samples versus their control counterparts resulted in outstanding differences (Fig. 1A). In fact, Principal Component Analysis (PCA) of the proteome data corresponding to the four biological repeats clearly separated control and viroid-infected samples (see Figures 2A and 2B in Supporting Information).

A total of 409 spots were statistically significant ($p \leq 0.05$, after FDR correction). Among them, 224 spots showed a significant difference in volume and were abundant enough to enable identification by mass spectrometry. After a final selection of 92 spots showing a high average ratio ($|ratio| \geq 2$), 80 of them were found to be up-regulated and the other 12 were down-regulated by CEVd infection. These spots were picked from gels (Fig. 1B) for identification.

We successfully identified 45 proteins (Table 1), and some of them were present on the gel as two or more spots, suggesting the existence of different isoforms and/or post-translational modifications producing the mobility shift in 2-D gels. Proteins were manually classified into different functional categories: defence response, transcription and translation, metabolism and energy, and other functions.

3.2. Validation by RT-PCR

In order to verify our 2-D DIGE results, a total of 18 genes coding for the most prominent proteins identified were selected for RT-PCR analysis (Table 1). Among these, pathogenesis related proteins PR1 and P23 were used as viroid infection markers [27, 28]. Figure S1 (Supporting Information) shows the densitogram corresponding to some representative differential proteins. Oligonucleotide primers for these 18 genes were designed,

and total RNA from control and CEVd-infected tomato plants was subjected to a qualitative RT-PCR analysis. According to the results obtained (Fig. 2), genes were classified into two expression groups. First group contained 6 genes with a very apparent change at the transcriptional level between control and CEVd-infected plants, whilst the second one corresponded to 12 genes with little or no difference at the mRNA level. All the proteins belonging to the first group were found to be integrated into the defence response category (Table 1), including the two reference proteins PR1 and P23, other pathogenesis related proteins like PR10 and P69G, and some defence proteins such as endochitinase and β-glucanase (Fig. 2A). All these are late-response genes, and they appear to be regulated mainly at the transcriptional level. On the other hand, genes showing no difference at the transcriptional level fell into all four of protein categories listed in Table 1. Thus, carbonic anhydrase, ascorbate peroxidase, Fe-superoxide dismutase and Cu-Zn-superoxide dismutase are defensive response proteins. Elongation factor eEF2, elongation factor 1-alpha (eEF1A), eukaryotic translation initiation factor 5A (eIF5A), ribosomal protein S3 and ribosomal protein L10 are involved in translation. Glyceraldehyde-3-phosphate dehydrogenase belongs to the group of metabolism and energy proteins. Finally, in the miscellaneous group, TGF-beta receptor-interacting protein 1 and xyloglucan endotransglycosylase LeXET2 were also tested. Among them, the translation factors were selected for further studies (Fig. 2B).

3.3. Induction of transcriptionally activated proteins by GA

Gentisic acid has been described as the most important metabolite induced by CEVd in tomato plants [18], and its exogenous application induces a set of PR proteins that are not induced by SA, which is its immediate precursor [14, 17], indicating that GA may act as a signal molecule for plant defence response in compatible interactions. Since tomato and CEVd display a compatible interaction, we considered the possible implication of GA in the

viroid-mediated induction of those proteins showing differences at the transcriptional level. To study this, tomato leaves were treated with SA, GA or water. Tissue samples were collected at different times and RT-PCR analysis from the corresponding RNAs was performed (Fig. 3). As expected, PR1 was induced by both SA and GA, while P23 was only induced by GA treatment [14]. The mRNA levels for pathogenesis related proteins PR10 and P69G were strongly increased by GA, whereas SA produced a lower effect in their pattern of mRNA accumulation.

Furthermore, β-glucanase mRNA was induced exclusively by GA. Accordingly with the lower induction of the endochitinase mRNA by CEVd (Fig. 2A), only a slight induction could be observed for this gene in GA-treated, but not in SA-treated plants. The above data indicate that the induction of mRNAs for these proteins in tomato by CEVd infection could be regulated mediated by GA, confirming the possible role of this molecule in the signalling of compatible plant-pathogen interactions.

3.4. CEVd-induced protein mobility shifts and CEVd-host protein complexes

Among the proteins induced by CEVd displaying no differences at the transcriptional level, eEF2, eEF1A and eIF5A were selected to perform Western blot analysis in order to verify the 2-D DIGE results. To avoid the interference of the RuBisCO large subunit with eEF1A (both proteins of ca. 50 kDa) and to improve the resolution of the immunological analysis, we used two-dimensional PAGE for the Western blot validations. Membranes containing electrotransferred proteins from control or infected leaves were incubated with either anti-eEF1A, anti-eEF2 or anti-eIF5A antisera (Fig. 4), and differences in immunostaining were qualitatively considered.

As expected for eEF1A and eEF2, the antibodies recognized the identified spots (numbered in Figure 1B as 405 and 294, respectively) in the 2-D Western, and a more intense

immunodecoration was observed in infected samples as compared to their corresponding spots from control plants. Moreover, antisera revealed new spots in the protein extracts from infected plants, thus suggesting that either some new isoforms were induced and/or posttranslational modifications could be occurring as a result of CEVd infection although a possible immuno cross-reaction cannot be ruled out.

As far as eIF5A is concerned, six different spots were detected in the 2-D Western blot corresponding to control plants, and three additional spots in protein samples from CEVd-infected plants, once again indicating the existence of different isoforms and/or post-translational modifications causing the shift in the 2-D mobility. To test this possibility, all spots were picked and identified by MALDI MS/MS and LC/MS/MS as described in Materials and Methods (see Figures 3A, 3B and 3C in Supporting Information for alignments). Because the spot 3 was very close to the PR-10 spot, we took it from the control gels for its identification; the rest of the spots were picked from infected, 2-D-resolved samples. As Table 2 shows, spots 1, 3 and 8 corresponded to different peptides of the isoform 3 of tomato eIF5A (eIF5A-3). In turn, spots 2, 5 and 7 corresponded to the eIF5A-4 isoform, whilst spots 4, 6 and 9 were identified as eIF5A-2. Therefore, each isoform appears to display two different isoelectric points in control uninfected plants. CEVd infection results in an additional mobility shift for these isoforms, with a higher isoelectric point and a lower molecular weight.

Our data indicates that some proteins showing no changes at the transcriptional level display different accumulation ratios upon viroid infection. Moreover, the change in the mobility of the different isoforms caused by CEVd infection suggests that the non-coding pathogen could be also provoking posttranslational modifications.

To detect possible interactions between these translation factors (eEF2, eEF1A and eIF5A) and the viroid RNA, we performed 2-D Northwestern analysis. To do that, samples

from infected tissues were resolved by 2-D PAGE in triplicate, and then the gels were used for silver-staining, Western blot and CEVd-hybridization, respectively. By doing this, a physical interaction between the eEF1A spot and the viroid RNA could be reproducibly detected (Figure 5). No significant interaction was found between the CEVd RNA and the other two translation factors, eEF2 and eIF5A.

4. Discussion

Viroids are non-coding pathogens that can infect a broad range of plants causing devastating diseases. How they can regulate the host gene expression through means other than encoding proteins for specific functions still remains unknown [5, 29]. In this sense, the proteomic analysis of viroid infected plants constitutes a new promising approach in order to better understand such a host-pathogen relationship.

In this work we used two-dimensional DIGE to widen the previous knowledge of the protein component associated with the response of tomato plants to the infection with *Citrus exocortis viroid* (CEVd). We have identified 45 differentially abundant proteins and classified them as belonging into different functional groups. The validation studies by RT-PCR and 2-D Western blot revealed two different behaviours. A first group of genes showed outstanding changes at the transcriptional level corresponding with changes in abundances of respective proteins (between control and infected plants). In contrast, the viroid infection provoked also posttranscriptional changes in the abundance of a second group of proteins, without altering the levels of the respective mRNAs. The later validates the use of proteomic approach in synergy with the transcriptome analysis..

Belonging to the first group of proteins being controlled at transcripcional level, we found the well-known pathogenesis-related proteins PR1 and P23 (used as classical viroid infection markers [27, 28]), as well as other defence proteins such as an endochitinase, a β-

glucanase and pathogenesis-related proteins P69G and PR10, which until now had not been implicated in a plant-viroid interaction. P69G is a recently described P69 isoform, which has been involved in resistance to fungi [30, 31]. In regards to several PR10 proteins, they have been reported as capable of an activity important in different plant-pathogen interactions – hydrolysis of RNA [32-35]. More specifically, the CaPR-10 from TMV-infected pepper can degrade viral RNA [34]. Similar studies have been performed in cotton, where GaPR-10 degrades fungal RNA as well as specific plant RNAs induced by the pathogen [33]. Furthermore, the tomato CEVd-induced PR10 protein could be able to degrade the viroid RNA, thus contributing to the plant defence response. The induction of the genes mentioned above confirms that the defence response is transcriptionally activated upon viroid infection. In fact, this group of genes, which share a common regulation pattern, could be classified as belonging to the PR-1 regulon according to Maleck *et al*. [36]. In *Arabidopsis*, this regulon contains PR genes and novel genes that function during the systemic acquired resistance, and may be de-repressed during the defence response [37].

We also studied the possible implication of gentisic acid (GA) in the induction of these defence proteins, since GA has been proposed as a signal molecule for plant defence response in compatible interactions [14, 17, 18]. In fact, we observed a strong induction of the β-glucanase, PR10, P69G and the GA-marker protein P23 [14] caused by GA treatments. Our results suggest that the induction of these proteins in tomato by CEVd could be mediated by GA.

Among the second group of proteins displaying no transcriptional difference between control and infected plants, we found that CEVd infection induced the accumulation of different ribosomal proteins and several translation factors. This suggests that, despite its lack of protein-coding capacity, the viroid seems to have the ability to interfere with the host translational machinery. In this respect, we have detected alterations in proteins from the 40S

ribosomal subunit, such as S3 and S5, and in the 60S ribosomal protein L10 (spots 746, 999 and 938/948). Several lines of evidence have related ribosomal proteins with virus and viroid infections. It has been described for the ribosomal protein rpL10A that the regulation of its trafficking to the nucleus represents a defence strategy of plant cells against virus [38]. The ribosomal protein rpS5 is a critical element in positioning the Hepatitis C Virus RNA on the 40S ribosomal subunit during translation initiation [39]. Recently, the interaction between the positive strand (+) of the Potato Spindle Tuber Viroid (PSTVd) and the ribosomal protein L5 from *Arabidopsis thaliana* has been reported [40]. Nevertheless, the precise implication of the ribosomal proteins in defence remains unknown.

The translation elongation factor 1A has been implicated in the replication of positive strand RNA virus of both plants and animals. This elongation factor interacts directly with the positive strand of the viral RNA or binds to the viral RNA-dependent RNA polymerase (RdRp) [41]. Factor 1A has also been proposed to facilitate the assembly of the tombusvirus replicase and to stimulate minus-strand synthesis [42]. The down-regulation of *eEF1A* mRNA levels by VIGS in *Nicotiana benthamiana* dramatically reduced the accumulation of TMV RNA and the spread of TMV infection [43]. Furthermore, an interaction between eEF1A from *Prunus persica* and the Peach Latent Mosaic Viroid (PLMVd) has been detected [26]. Here we show evidence on this eEF1A-viroid interaction between the tomato eEF1A and the *Citrus exocortis viroid.*

Factor eIF5A has been involved in pathogen-induced cell death and development of disease symptoms in *Arabidopsis*. Specifically, the antisense *AteIF5A-2* plants exhibited a marked resistance to colonization by virulent *Pseudomonas syringae* pv *tomato* DC3000. Strikingly, AteIF5A-2-overexpressing *Arabidopsis* plants display stunted growth and also showed chlorotic and curled leaves [44], which coincide with the classical symptoms of viroid

disease. This points out to the possibility that the induction of eIF5A in tomato by CEVd infection could be somehow related with the appearance of symptoms.

Eukaryotic elongation factor 2 is a GTPase that catalyzes the translocation of the peptidyl tRNA from the A site to the P site of the ribosome during translation. Maize eEF2 has been found to undergo an increased phosphorylation in root tissues subjected to oxygen deprivation [45], but little is known about its implication in plant-pathogen interactions. However, in monkey kidney cells infected with African Swine Fever Virus, eEF2 factor has been found to be enriched in areas surrounding virus factories [46], and to concentrate where viral RNA replication occurs in hamster kidney cells infected with Sindbis Virus [47]. On the other hand, it has been implicated in the programmed ribosomal frame shifting that takes place in the replication of numerous viral pathogens [48]. To the best of our knowledge, this is the first time that eEF2 factor has been proposed to be involved in plant pathogenesis.

Eukaryotic translation initiation factor 5A interacts with the structural components of the 80S ribosome complex, as well as with the translation elongation factors eEF1A and eEF2 [49, 50]. Since we have detected an interaction between eEF1A and CEVd, this could be part of a bigger complex including eIF5A and eEF2. If this were the case, the eEF1A-CEVd complexes could also be recruiting eIF5A and eEF2, thus forcing the cell to increase the amount of these translation factors to try to overcome their displacement by the viroid and guarantee their normal function.

We have also detected the appearance of new spots recognised by the corresponding antibodies against the elongation factors 1 and 2 (eEF1A and eEF2) as a consequence of the viroid infection (Fig. 4). Three covalent protein modifications are exceptional in the fact that they have been so far detected only on these proteins: ethanolamine phosphoglycerol attached to glutamic acid residues on eEF1A, histidine residues modified as diphthamide on eEF2, and hypusinations of lysine residues on eIF5A. The proteins carrying these modifications are all

involved in elongation steps of translation [51]. Our results circumstantially indicate that the viroid could be somehow interfering with these highly conserved factors by altering their posttranslational modifications. Related to this, it has been reported that the expression of the AteIF5A-2 protein appears to be posttranscriptionally regulated upon *Pseudomonas syringae* infection, resulting in a faster migration of the band in SDS-PAGE in Arabidopsis infected plants [44]. Furthermore, the importance of diphthamide modification in eEF2 function may become apparent during stress conditions [52]. Other posttranslational modification on eEF2, such as phosphorylation, has been shown to be promoted by Avian Reovirus in monkey kidney epithelial cells [53]. Finally, the activity of eEF1A is modulated by different posttranslational modifications but the precise role of these modifications still remains unclear [51].

Our results indicate that the CEVd, a non-coding pathogen, interferes with the translation machinery of the host as a part of the plant-pathogen interaction. The survival of cells exposed to adverse environmental conditions requires a radical reprogramming of protein translation [54]. Thus, viroid infection may alter the normal function of the translation machinery, so that the cells would adapt to the new stress conditions.

Because of their RNA nature, a number of previous studies have focused on the involvement of viroids in RNA-mediated transcriptional and posttranscriptional gene silencing [55] but less is known about their effect on the translational machinery. Using proteomics technology, the present report follows a complementary approach to understand viroid pathogenesis, and provides new information that points out to various translation-related proteins that are affected at the translational and posttranscription level. Therefore, the role of viroids in plant pathogenesis should be understood as a complex interaction between these small, non-coding RNAs and critical cell processes of transcription and translation.

References

[1] Flores, R., Hernandez, C., de Alba, A. E. M., Daros, J. A., Di Serio, F., *Annual Review of Phytopathology* 2005, pp. 117-139.
[2] Ding, B., Itaya, A., Viroid: A useful model for studying the basic principles of infection and RNA biology. *Molecular Plant-Microbe Interactions* 2007, *20*, 7-20.
[3] Ding, B., Kwon, M. O., Hammond, R., Owens, R., Cell-to-cell movement of potato spindle tuber viroid. *Plant Journal* 1997, *12*, 931-936.
[4] Zhu, Y. L., Green, L., Woo, Y. M., Owens, R., Ding, B., Cellular basis of potato spindle tuber viroid systemic movement. *Virology* 2001, *279*, 69-77.
[5] Qi, Y. J., Pelissier, T., Itaya, A., Hunt, E., *et al.*, Direct role of a viroid RNA motif in mediating directional RNA trafficking across a specific cellular boundary. *Plant Cell* 2004, *16*, 1741-1752.
[6] Flores, R., Grubb, D., Elleuch, A., Nohales, M.-A., *et al.*, Rolling-circle replication of viroids, viroid-like satellite RNAs and hepatitis delta virus Variations on a theme. *Rna Biology* 2011, *8*, 200-206.
[7] Ding, B., The biology of viroid-host interactions. *Annual Review of Phytopathology* 2009, pp. 105-131.
[8] Granell, A., Bellés, J. M., Conejero, V., Induction of pathogenesis-related proteins in tomato by citrus exocortis viroid, silver ion and ethephon. *Physiological and Molecular Plant Pathology* 1987, *31*, 83-90.
[9] Vera, P., Conejero, V., Pathogenesis-related proteins of tomato P-69 as an alkaline endoproteinase. *Plant Physiology* 1988, *87*, 58-63.
[10] García-Breijo, F. J., Garro, R., Conejero, V., C7(P32) and C6(P34) PR proteins induced in tomato leaves by citrus exocoris viroid infection are chitinases. *Physiological and Molecular Plant Pathology* 1990, *36*, 249-260.
[11] Domingo, C., Conejero, V., Vera, P., Genes encoding acidic and basic class-III beta-1,3-glucanases are expressed in tomato plants upon viroid infection. *Plant Molecular Biology* 1994, *24*, 725-732.
[12] Bellés, J. M., Granell, A., Duranvila, N., Conejero, V., ACC synthesis as the activated step responsible for the rise of ethylene production accompanying citrus exocortis viroid infection in tomato plants *Journal of Phytopathology* 1989, *125*, 198-208.
[13] Bellés, J. M., Perezamador, M. A., Carbonell, J., Conejero, V., Correlation between ornithine decarboxylase and putrescine in tomato plants infected by citrus-exocortis viroid or treated with ethephon. *Plant Physiology* 1993, *102*, 933-937.
[14] Bellés, J. M., Garro, R., Fayos, J., Navarro, P., *et al.*, Gentisic acid as a pathogen-inducible signal, additional to salicylic acid for activation of plant defenses in tomato. *Molecular Plant-Microbe Interactions* 1999, *12*, 227-235.
[15] Fayos, J., Belles, J. M., Lopez-Gresa, M. P., Primo, J., Conejero, V., Induction of gentisic acid 5-O-beta-D-xylopyranoside in tomato and cucumber plants infected by different pathogens. *Phytochemistry* 2006, *67*, 142-148.
[16] Tárraga, S., Lisón, P., López-Gresa, M. P., Torres, C., *et al.*, Molecular cloning and characterization of a novel tomato xylosyltransferase specific for gentisic acid. *Journal of Experimental Botany* 2010, *61*, 4325-4338.
[17] Bellés, J. M., Garro, R., Pallas, V., Fayos, J., *et al.*, Accumulation of gentisic acid as associated with systemic infections but not with the hypersensitive response in plant-pathogen interactions. *Planta* 2006, *223*, 500-511.

[18] López-Gresa, M. P., Maltese, F., Bellés, J. M., Conejero, V., *et al.*, Metabolic response of tomato leaves upon different plant-pathogen interactions. *Phytochemical Analysis* 2010, *21*, 89-94.
[19] Eggert, K., Pawelzik, E., Proteome analysis of Fusarium head blight in grains of naked barley (Hordeum vulgare subsp. nudum). *Proteomics* 2011, *11*, 972-985.
[20] Li, Y., Zhang, Z., Nie, Y., Zhang, L., Wang, Z., Proteomic analysis of salicylic acid induced resistance to magnaporthe oryzae in susceptible and resistant rice. *Proteomics* 2012.
[21] Xu, Q.-F., Cheng, W.-S., Li, S.-S., Li, W., *et al.*, Identification of genes required for Cf-dependent hypersensitive cell death by combined proteomic and RNA interfering analyses. *Journal of Experimental Botany* 2012, *63*, 2421-2435.
[22] Castillejo, M. A., Fernandez-Aparicio, M., Rubiales, D., Proteomic analysis by two-dimensional differential in gel electrophoresis (2D DIGE) of the early response of Pisum sativum to Orobanche crenata. *Journal of Experimental Botany* 2012, *63*, 107-119.
[23] Badillo-Vargas IE, R. D., Schneweis DJ, Hiromasa Y, Tomich JM, Whitfield AE, Proteomic analysis of Frankliniella occidentalis and differentially-expressed proteins in response to Tomato spotted wilt virus infection *Journal of Virology* 2012, *13*.
[24] Bellés, J. M., Carbonell, J., Conejero, V., Polyamines in plants infected by citrus-exocortis viroid or treated with silver ions and ethephon. *Plant Physiology* 1991, *96*, 1053-1059.
[25] Shevchenko, A., Jensen, O. N., Podtelejnikov, A. V., Sagliocco, F., *et al.*, Linking genome and proteome by mass spectrometry: Large-scale identification of yeast proteins from two dimensional gels. *Proceedings of the National Academy of Sciences of the United States of America* 1996, *93*, 14440-14445.
[26] Dubé, A., Bisaillon, M., Perreault, J.-P., Identification of proteins from *Prunus persica* that interact with peach latent mosaic viroid. *Journal of Virology* 2009, *83*, 12057-12067.
[27] Rodrigo, I., Vera, P., Frank, R., Conejero, V., Identification of the viroid-induced tomato pathogenesis-related (PR) protein P23 as the thaumatin-like tomato protein NP24 associated with osmotic-stress. *Plant Molecular Biology* 1991, *16*, 931-934.
[28] Tornero, P., Gadea, J., Conejero, V., Vera, P., Two PR-1 genes from tomato are differentially regulated and reveal a novel mode of expression for a pathogenesis-related gene during the hypersensitive response and development. *Molecular Plant-Microbe Interactions* 1997, *10*, 624-634.
[29] Takeda, R., Ding, B., Viroid intercellular trafficking: RNA motifs, cellular factors and broad impacts. *Viruses-Basel* 2009, *1*, 210-221.
[30] Kavroulakis, N., Ntougias, S., Zervakis, G. I., Ehaliotis, C., *et al.*, Role of ethylene in the protection of tomato plants against soil-borne fungal pathogens conferred by an endophytic *Fusarium solani* strain. *Journal of Experimental Botany* 2007, *58*, 3853-3864.
[31] Larson, R. L., Hill, A. L., Nunez, A., Characterization of protein changes associated with sugar beet (*Beta vulgaris*) resistance and susceptibility to *Fusarium oxysporum*. *Journal of Agricultural and Food Chemistry* 2007, *55*, 7905-7915.
[32] Swoboda, I., HoffmannSommergruber, K., Oriordain, G., Scheiner, O., *et al.*, Bet v 1 proteins, the major birch pollen allergens and members of a family of conserved pathogenesis-related proteins, show ribonuclease activity in vitro. *Physiologia Plantarum* 1996, *96*, 433-438.
[33] Zhou, X. J., Lu, S., Xu, Y. H., Wang, J. W., Chen, X. Y., A cotton cDNA (GaPR-10) encoding a pathogenesis-related 10 protein with in vitro ribonuclease activity. *Plant Science* 2002, *162*, 629-636.
[34] Park, C. J., Kim, K. J., Shin, R., Park, J. M., *et al.*, Pathogenesis-related protein 10 isolated from hot pepper functions as a ribonuclease in an antiviral pathway. *Plant Journal* 2004, *37*, 186-198.

[35] Chen, Z. Y., Brown, R. L., Rajasekaran, K., Damann, K. E., Cleveland, T. E., Identification of a maize kernel pathogenesis-related protein and evidence for its involvement in resistance to Aspergillus flavus infection and aflatoxin production. *Phytopathology* 2006, *96*, 87-95.
[36] Maleck, K., Levine, A., Eulgem, T., Morgan, A., *et al.*, The transcriptome of *Arabidopsis thaliana* during systemic acquired resistance. *Nature Genetics* 2000, *26*, 403-410.
[37] Lodha, T., Basak, J., Plant–Pathogen Interactions: What Microarray Tells About It? *Molecular Biotechnology* 2011, 1-11.
[38] Carvalho, C. M., Santos, A. A., Pires, S. R., Rocha, C. S., *et al.*, Regulated nuclear trafficking of rpL10A mediated by NIK1 represents a defense strategy of plant cells against virus. *Plos Pathogens* 2008, *4*.
[39] Fukushi, S., Okada, M., Stahl, J., Kageyama, T., *et al.*, Ribosomal protein S5 interacts with the internal ribosomal entry site of hepatitis C virus. *Journal of Biological Chemistry* 2001, *276*, 20824-20826.
[40] Eiras, M., Angeles Nohales, M., Kitajima, E. W., Flores, R., Antonio Daros, J., Ribosomal protein L5 and transcription factor IIIA from Arabidopsis thaliana bind in vitro specifically Potato spindle tuber viroid RNA. *Archives of Virology* 2011, *156*, 529-533.
[41] Mateyak, M. K., Kinzy, T. G., eEF1A: Thinking outside the ribosome. *Journal of Biological Chemistry* 2010, *285*, 21209-21213.
[42] Li, Z., Pogany, J., Tupman, S., Esposito, A. M., *et al.*, Translation elongation factor 1A facilitates the assembly of the tombusvirus replicase and stimulates minus-strand synthesis. *Plos Pathogens* 2010, *6*.
[43] Yamaji, Y., Sakurai, K., Hamada, K., Komatsu, K., *et al.*, Significance of eukaryotic translation elongation factor 1A in tobacco mosaic virus infection. *Archives of Virology* 2010, *155*, 263-268.
[44] Hopkins, M. T., Lampi, Y., Wang, T.-W., Liu, Z., Thompson, J. E., Eukaryotic translation initiation factor 5A is involved in pathogen-induced cell death and development of disease symptoms in Arabidopsis. *Plant Physiology* 2008, *148*, 479-489.
[45] Szick-Miranda, K., Jayachandran, S., Tam, A., Werner-Fraczek, J., *et al.*, Evaluation of translational control mechanisms in response to oxygen deprivation in maize. *Russian Journal of Plant Physiology* 2003, *50*, 774-786.
[46] Castelló, A., Quintas, A., Sanchez, E. G., Sabina, P., *et al.*, Regulation of Host Translational Machinery by African Swine Fever Virus. *Plos Pathogens* 2009, *5*.
[47] Sanz, M. A., Castelló, A., Ventoso, I., Berlanga, J. J., Carrasco, L., Dual Mechanism for the Translation of Subgenomic mRNA from Sindbis Virus in Infected and Uninfected Cells. *Plos One* 2009, *4*.
[48] Namy, O., Moran, S. J., Stuart, D. I., Gilbert, R. J. C., Brierley, I., A mechanical explanation of RNA pseudoknot function in programmed ribosomal frameshifting. *Nature* 2006, *441*, 244-247.
[49] Jao, D. L. E., Chen, K. Y., Tandem affinity purification revealed the hypusine-dependent binding of eukaryotic initiation factor 5A to the translating 80S ribosomal complex. *Journal of Cellular Biochemistry* 2006, *97*, 583-598.
[50] Zanelli, C. F., Maragno, A. L. C., Gregio, A. P. B., Komili, S., *et al.*, eIF5A binds to translational machinery components and affects translation in yeast. *Biochemical and Biophysical Research Communications* 2006, *348*, 1358-1366.
[51] Greganova, E., Altmann, M., Buetikofer, P., Unique modifications of translation elongation factors. *Febs Journal* 2011, *278*, 2613-2624.
[52] Gupta, P. K., Liu, S., Batavia, M. P., Leppla, S. H., The diphthamide modification on elongation factor-2 renders mammalian cells resistant to ricin. *Cellular Microbiology* 2008, *10*, 1687-1694.

[53] Ji, W. T., Wang, L., Lin, R. C., Huang, W. R., Liu, H. J., Avian reovirus influences phosphorylation of several factors involved in host protein translation including eukaryotic translation elongation factor 2 (eEF2) in Vero cells. *Biochemical and Biophysical Research Communications* 2009, *384*, 301-305.
[54] Yamasaki, S., Anderson, P., Reprogramming mRNA translation during stress. *Current Opinion in Cell Biology* 2008, *20*, 222-226.
[55] Sano, T., Barba, M., Li, S.-F., Hadidi, A., Viroids and RNA silencing: mechanism, role in viroid pathogenicity and development of viroid-resistant plants. *GM crops* 2010, *1*, 80-86.

Acknowledgments

We would like to thank the Proteomic Service of the IBMCP (Instituto de Biología Molecular y Celular de Plantas, Valencia, Spain) for the technical assistance. We also thank Dr. Alejandro Ferrando (Instituto de Biología Molecular y Celular de Plantas UPV-CSIC) for critical reading of the manuscript, discussions, and for kindly providing us with the eIF5A antisera. We are also grateful to Dr. Brenda Hunter (University of Arizona) for both eEF1A and eEF2 antiserum. This work was supported by Grant BFU2009-11958 from Dirección General de Programas y Transferencia de Conocimiento, from Spanish Ministry of Science and Innovation. Laura Campos was the recipient of a predoctoral fellowship ACIF/2010/231 from Generalitat Valenciana (Spain). Mª Pilar López-Gresa held a postdoctoral fellowship JAEDoc_08_00402 from the Consejo Superior de Investigaciones Científicas (Spain).

Figure Legends

Figure 1. Analysis by 2-D DIGE of tomato leaf proteins. Equal amounts (50 μg) of control sample (Cy5-labelled, red), viroid-infected sample (Cy3-labelled, green) and internal standard (Cy2-labelled, blue) were loaded in the same gel. (A) Overlay of the three fluorescence images. Proteins induced by viroid infection appear in green, those repressed appear in red, and proteins unaffected appear in white. (B) DeCyder image corresponding to the Cy2 dye (internal standard) for the same gel shown in Figure 1A. Proteins picked for sequencing are outlined in red. Proteins with a positive sequence identification are also tagged with their respective numbers, which correspond to the same ones shown in Table 1.

Figure 2. Validation of 2-D-DIGE results by RT-PCR. RNAs from four biological replicates (R1 to R4) of control (left) and CEVd-infected (right) tomato plants were used to perform RT-PCR by using specific primers designed for the following gene sequences: (A) PR1, P23, PR10, P69G, β-glucanase and endochitinase, and (B) eIF5A-3, eEF1-A and eEF2. Leaf tissue was collected 20 days after viroid inoculation. The corresponding spot number is indicated in each case.

Figure 3. Proteins transcriptionally activated by CEVd infection also exhibit mRNA accumulation when treated by gentisic acid or salicylic acid. Tomato leaves treated either with salicylic acid (SA), gentisic acid (GA) or water were collected at different time points (0, 1, 4, 8 and 24 hours after treatment),then total RNA was extracted and used to perform RT-PCR by using specific primers designed for the following genes: PR1, P23, PR10, P69G, β-glucanase and endochitinase. The corresponding spot number is indicated in each case.

Figure 4. 2-D Western blots. The figure is a composite of six different membranes, corresponding to protein extracts from control or CEVd-infected tomato leaves, either incubated with anti-eEF1A, anti-eEF2 or anti-eIF5A. (A) Assembled immunodetected areas for eEF1A, eEF2 and eIF5A in the control extracts. (B) Assembled immunodetected areas for eEF1A, eEF2 and eIF5A in the CEVd-infected extracts.

Figure 5. Binding of viroid RNA to the eEF1A protein. Proteins from CEVd-infected plants were separated by 2-D PAGE and transferred to nitrocellulose. The membrane was incubated with a radiolabelled RNA transcript of the CEVd sequence and exposed to X-Ray films. Panels show the area surrounding the eEF1A spot. The panel on the left corresponds to the silver-stained gel. The central panel shows the position of the eEF1A protein as revealed by immunoblot. The panel on the right corresponds to the autoradiography of the membrane incubated with radiolabelled viroid RNA.

TABLE 1. List of identified proteins

	Spot [a]	Protein/function [b]	Accession [c]	Species	MW [d]	p*I* [e]	Ratio	*p*-value [f]	score / sequence coverage (%) / peptides matched
		Defense Response							
	132	Pathogenesis related protein P69B	CAA71234.1 (1)	*Solanum lycopersicum*	78931	6,53	2,00	0,0400	133 / 42 / 18
I	174	Pathogenesis related protein P69G	AAZ81612.1 (1)	*Solanum lycopersicum*	37812	7,01	16,48	0,0024	532 / 40 / 11
	175	Pathogenesis related protein P69C	CAA06412.1 (1)	*Solanum lycopersicum*	80121	8,25	11,79	0,0038	402 / 10 / 8
	682	Osmotin-like protein OSML13	P50701.1 (2)	*Solanum commersonii*	26654	6,88	2,82	0,0160	80 / 33 / 5
I	695	Glucan endo-1,3-beta-glucosidase B	Q01413.1 (2)	*Solanum lycopersicum*	39719	8,10	11,68	0,0064	354 / 25 / 7
	696	Glucan endo-1,3-beta-glucosidase B	Q01413.1 (2)	*Solanum lycopersicum*	39719	8,10	2,86	0,0066	63 / 13 / 4
	788	Glucan endo-1,3-beta-glucosidase B	Q01413.1 (2)	*Solanum lycopersicum*	39719	8,10	5,08	0,0290	136 / 16 / 4
I	791	Basic 30 kDa endochitinase	Q05538.1 (2)	*Solanum lycopersicum*	34346	6,45	9,23	0,0084	83 / 38 / 8
I	830	Carbonic anhydrase	CAH60891.1 (1)	*Solanum lycopersicum*	34468	6,97	2,96	0,0038	374 / 26 / 9
I	896	Cytosolic ascorbate peroxidase 1	AAZ77770.1 (1)	*Solanum lycopersicum*	27408	5,76	4,40	0,0014	102 / 70/ 11
	983	Glucan endo-1,3-beta-glucosidase B	Q01413.1 (2)	*Solanum lycopersicum*	39719	8,10	3,63	0,0150	67 / 17 / 4
I	984	Pathogenesis related protein P23	X70787.1 (1)	*Solanum lycopersicum*	26646	7,91	14,14	0,0028	88 / 25 / 5
I	1011	Superoxide dismutase [Fe]	CAE22480.1 (1)	*Solanum lycopersicum*	27911	6,97	3,68	0,0011	350 / 33 / 9
I	1138	Pathogenesis-related protein 10	AAU00066.1 (1)	*Solanum virginianum*	17587	5,33	4,14	0,0190	120 / 14 / 2
I	1286	Superoxide dismutase [Cu-Zn], chloroplastic	P14831.1 (2)	*Solanum lycopersicum*	22228	6,04	5,31	0,0027	138 / 17 / 3
I	1333	Pathogenesis related protein PR1	X68738.1 (1)	*Solanum lycopersicum*	14862	8,96	2,85	0,0088	87 / 56 / 6
		Replication, transcription and translation							
I	294	Elongation factor EF-2	BAB86847.1 (1)	*Pisum sativum*	55032	5,99	4,08	0,0021	530 / 38 / 13
I	405	Elongation factor 1-alpha	P17786.1 (2)	*Solanum lycopersicum*	49288	9,14	2,13	0,0088	144 / 27 / 10
I	746	40S ribosomal (S3)-like protein, clone 084G12	DQ294256.1 (1)	*Solanum tuberosum*	26394	9,52	3,06	0,0056	128 / 48 / 9
	792	Ribosomal protein S6	CAA48187.1 (1)	*Nicotiana tabacum*	21784	10,79	2,55	0,0360	52 / 6 / 1
	796	Putative cyclin-dependent kinase F-2	Q2QSL4.1 (2)	*Oryza sativa*	35622	7,72	3,12	0,0030	43 / 33 / 7
	854	DEAD-box ATP-dependent RNA helicase 26	Q0JL73.1 (2)	*Oryza sativa*	58849	9,44	7,76	0,0038	41 / 27 / 9
	938	60S ribosomal protein L10	Q9M5M7.1 (2)	*Euphorbia esula*	24947	10,59	5,25	0,0011	263 / 28 / 6
I	948	60S ribosomal protein L10	Q9M5M7.1 (2)	*Euphorbia esula*	24947	10,59	6,29	0,0070	159 / 24 / 4
	956	DNA replication licensing factor MCM3 homolog 1	Q43704.2 (2)	*Zea mays*	85182	6,08	10,84	0,0039	34 / 12/ 7
	999	40S ribosomal protein S5	O65731.1 (2)	*Cicer arietinum*	22018	9.93	7,90	0,0048	277 / 33 / 6
	1145	RNA polymerase subunit	AAB00528.1 (1)	*Arabidopsis thaliana*	41793	5,53	-2,68	0,0068	50 / 4 / 2
I	1162	Eukaryotic translation initiation factor 5A-2	P24922.1 (2)	*Nicotiana plumbaginifolia*	17364	5,76	4,33	0,0061	61 / 11 / 2
		Metabolism and energy							
	511	Rubisco activase, chloroplastic	O49074.1 (2)	*Solanum pennellii*	50701	8,48	-2,73	0,0150	77 / 17 / 7
	518	Rubisco activase, chloroplastic	O49074.1 (2)	*Solanum pennellii*	50701	8,48	-7,05	0,0094	426 / 50 / 25
	520	Rubisco activase, chloroplastic	O49074.1 (2)	*Solanum pennellii*	50701	8,48	-5,76	0,0031	440 / 48 / 23
	703	Oxygen-evolving enhancer protein 2 (OEE2), chloroplastic	P29795.1 (2)	*Solanum lycopersicum*	27792	8,18	2,16	0,0043	207 / 34 / 6
I	846	Glyceraldehyde-3-phosphate dehydrogenase (GAPDH), cytosolic	P26519.1 (2)	*Petroselinum crispum*	36372	7,37	9,12	0,0018	83 / 5 / 1
	878	Putative IPP isomerase	BAB16690.2 (1)	*Eucommia ulmoides*	25956	4,85	8,18	0,0009	97 / 14 / 3
	974	Oxygen-evolving enhancer protein 2 (OEE2), chloroplastic	P29795.1 (2)	*Solanum lycopersicum*	27792	8,18	-2,58	0,0110	77 / 39 / 7
	980	Oxygen-evolving enhancer protein 2 (OEE2), chloroplastic	P93566.1 (2)	*Solanum tuberosum*	28004	8,19	-2,27	0,0084	324 / 44 / 8
	1382	Photosystem II oxygen-evolving complex protein 3 (OEE3)	AAU03361.1 (1)	*Solanum lycopersicum*	24572	9,66	3,03	0,0043	132 / 27 / 8
	1469	Rubisco activase, chloroplastic	O49074.1 (2)	*Solanum pennellii*	50701	8,48	-3,21	0,0012	389 / 47 / 25
	1477	Triose phosphate isomerase cytosolic isoform	AAR11379.1 (1)	*Solanum chacoense*	27040	5,83	2,49	0,0084	109 / 11 / 2
		Other							
	483	Shoot/meristem cDNA clone cTOF22H3	BG128858.1 (1)	*Solanum lycopersicum*	25855	5,53	-4,03	0,0009	125 / 30 / 7
	501	Shoot/meristem cDNA clone cTOF19E1	BG128109.1 (1)	*Solanum lycopersicum*	25136	4,46	-2,08	0,0033	114 / 50 / 6
	607	TGF-beta receptor-interacting protein 1	AAK49947.1 (1)	*Phaseolus vulgaris*	35876	7,18	2,32	0,0011	184 / 12 / 4
I	609	TGF-beta receptor-interacting protein 1	AAK49947.1 (1)	*Phaseolus vulgaris*	35876	7,18	4,02	0,0011	50 / 4 / 1
I	777	Xyloglucan endotransglycosylase LeXET2	AAG00902.1 (1)	*Solanum lycopersicum*	31587	8,37	2,77	0,0210	200 / 16 / 4
	1014	SKP1 component, SFC ubiquitin ligase	AAT99735.1 (1)	*Nicotiana tabacum*	17528	4,42	-4,90	0,0014	50 / 36 / 5

(a) Assigned spot number as indicated in Fig. 1B. Black dots indicate the proteins selected for further studies.
(b) Identified protein of *S. lycopersicum* or homologous protein from other plants.
(c) Accesion number code refers to (1) GenBank or (2) SwissProt.
(d) Theoretical MW
(e) Theoretical p*I*
(f) *p*-value obteined form *t*-test including data from four biological replicates.

TABLE 2

Spot	Control	CEVd	Sequence
1162-1 1162-3	+	+	eIF5A-3
1162-8	-	+	
1162-2 1162-5	+	+	eIF5A-4
1162-7	-	+	
1162-4 1162-6	+	+	eIF5A-2
1162-9	-	+	

Table 2. Tomato eIF5A isoforms. Amino acid sequence correspondence between spots 1 to 9 from Figure 4B and different tomato eIF5A isoforms. Spots were picked from 2-D gels and identified by mass spectrometry. The presence (+) or absence (-) of each spot is indicated for control and CEVd-infected plant extracts.

SUPPORTING INFORMATION

1. Fluorescent labelling

Protein samples were labelled using the CyDyes DIGE fluorescent dyes (Cy2, Cy3 and Cy5) according to the manufacturer's instructions (GE Healthcare). Three different protein samples (internal standard, control and infected) were labelled separately with the three dyes. The internal standard was created by pooling aliquots of all biological samples analyzed in the experiment and was labelled with Cy2. Since four biological replicates were analyzed in this experiment, then 8 biological samples were used to make the internal standard. The control samples and the samples from CEVd-infected plants were alternatively labelled with Cy3 or Cy5, depending on the biological replicate, thus avoiding the label effect. Equal amounts (50 μg) of control (Cy3, for example), infected (Cy5) and internal standard (Cy2) samples of the same biological replicate were pooled. Lysis buffer was added to a final volume of 40 μL. Then, the sample was mixed with 40 μL of isoelectrofocusing (IEF) rehydration buffer (8 M urea, 4% CHAPS, 0.005% bromophenol blue) containing 65 mM DTT and 1% IPG buffer, pH 3-11, and loaded on the gel, making one gel per each biological replicate.

2. 2-D electrophoresis

For 2-D analysis, 24-cm long strips bearing an immobilized pH gradient from 3 to 11 were hydrated overnight at room temperature with 450 μL of IEF rehydration buffer, containing the reagents Destreak and Pharmalyte pH 3-10 (GE Healthcare). CyDyes-labelled samples (150 μg of protein) were loaded into the hydrated strips. IEF was performed on an IPGphor unit (GE Healthcare) at 20 ºC and a maximum current setting of 50 μA per strip, using the following settings: 300 V for 1 h, an increasing voltage gradient to 1000 V (6 h) and an increasing voltage

gradient to 8000 V (3 h) before finally holding at 8000 V for a total of 32000 volt-hours. After IEF, each strip was equilibrated separately for 15 min in 10 mL equilibration solution I (0.05 M Tris-HCl buffer, pH 8.8 containing 6 M urea, 30% glycerol, 2% SDS, 200 mg DTT per 10 mL buffer) followed by equilibration solution II (substituting DTT for 250 mg iodoacetamide per 10 mL buffer and adding 0.01% bromophenol blue) before being applied directly to the second dimension 12.5 % SDS-PAGE gels. Four gels were run simultaneously at 20 °C, applying 2W/gel for 30 min and 20 W/gel for the remaining 5-6 h, using an Ettan DALTsix unit (GE Healthcare). Running buffer consisted of 25 mM Tris, pH 8.3, 192 mM glycine and 0.2% SDS.

3. Gel imaging and data analysis

After SDS-PAGE, CyDye-labelled proteins were visualized by fluorescence scanning using a Typhoon Trio scanner (GE Healthcare) with the wavelengths corresponding to each CyDye. Cy2 images were scanned using a blue laser (488 nm) and a 520 nm band-pass (BP) 40 emission filter. Cy3 images were scanned using a green laser (532 nm) and a 580 nm BP 30 emission filter. Cy5 images were scanned using a red laser (633 nm) and a 670 nm BP 30 emission filter. All gels were scanned at 200 μm pixel size resolution. The photomultiplier tube was set between 500 to 600 V using normal sensitivity.

4. MALDI MS/MS and/or LC/MS/MS analyses

The digestion mixture was dried in a vacuum centrifuge, resuspended in 7 μL of 0.1% TFA (trifluoroacetic acid, Sigma), and 1 μL was spotted onto the MALDI target plate. After the droplets were air-dried at room temperature, 0.5 μL of matrix (5 mg/mL of CHCA in 0.1% TFA-ACN/H_2O (1:1, v/v) was added and allowed to air-dry at room temperature.

Figure 1

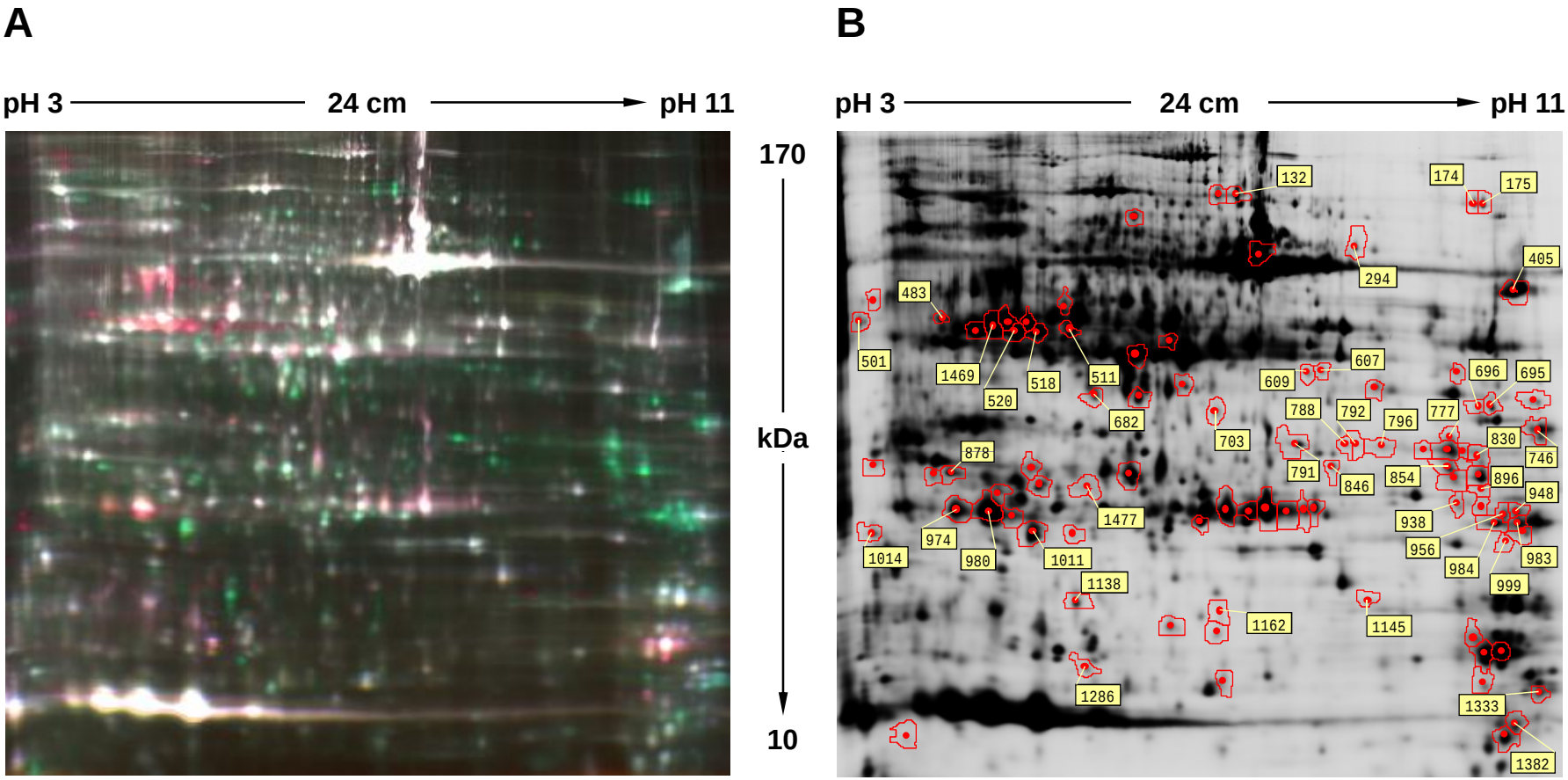
A
pH 3
24 cm
pH 11
170
kDa
10
B
pH 3
24 cm
pH 11
132
174
175
405
294
483
501
1469
520
518
511
682
609
607
703
788
792
796
777
696
695
830
746
878
791
846
854
896
948
1477
938
974
956
1014
980
1011
984
983
1138
999
1162
1145
1286
1333
1382

Figure 2

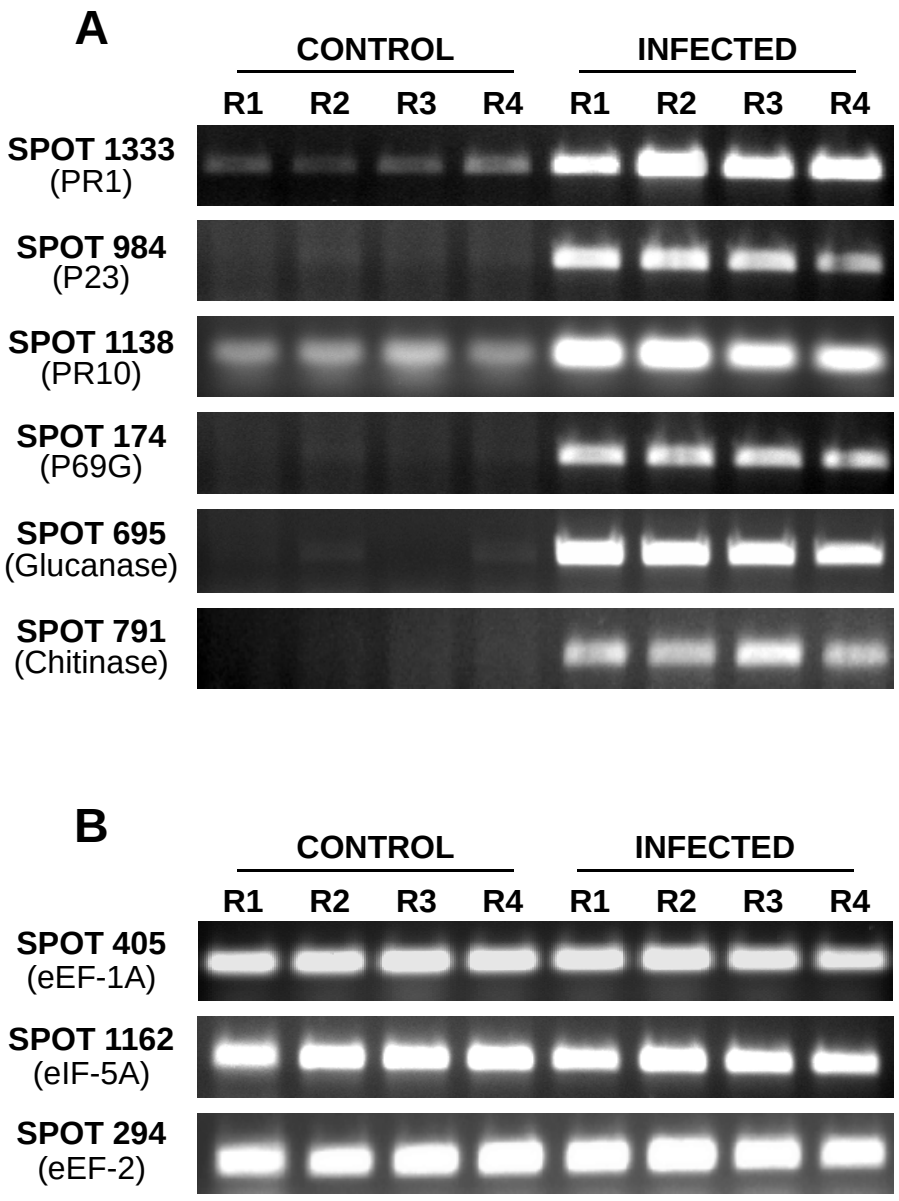
A
CONTROL
INFECTED
R1 R2 R3 R4 R1 R2 R3 R4
SPOT 1333
(PR1)
SPOT 984
(P23)
SPOT 1138
(PR10)
SPOT 174
(P69G)
SPOT 695
(Glucanase)
SPOT 791
(Chitinase)
B
CONTROL
INFECTED
R1 R2 R3 R4 R1 R2 R3 R4
SPOT 405
(eEF-1A)
SPOT 1162
(eIF-5A)
SPOT 294
(eEF-2)

Figure 3

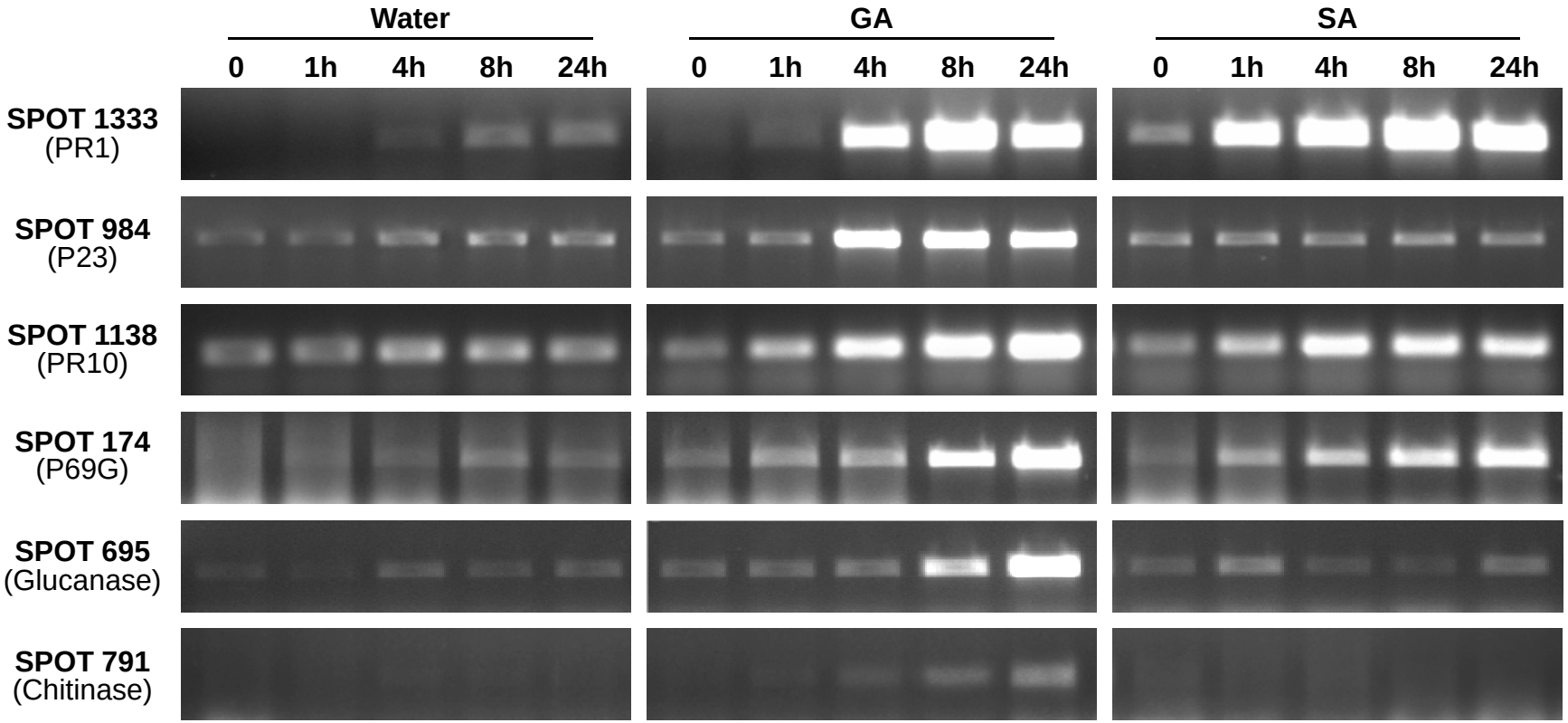
Water
GA
SA
0
1h
4h
8h
24h
SPOT 1333
(PR1)
SPOT 984
(P23)
SPOT 1138
(PR10)
SPOT 174
(P69G)
SPOT 695
(Glucanase)
SPOT 791
(Chitinase)

Figure 4

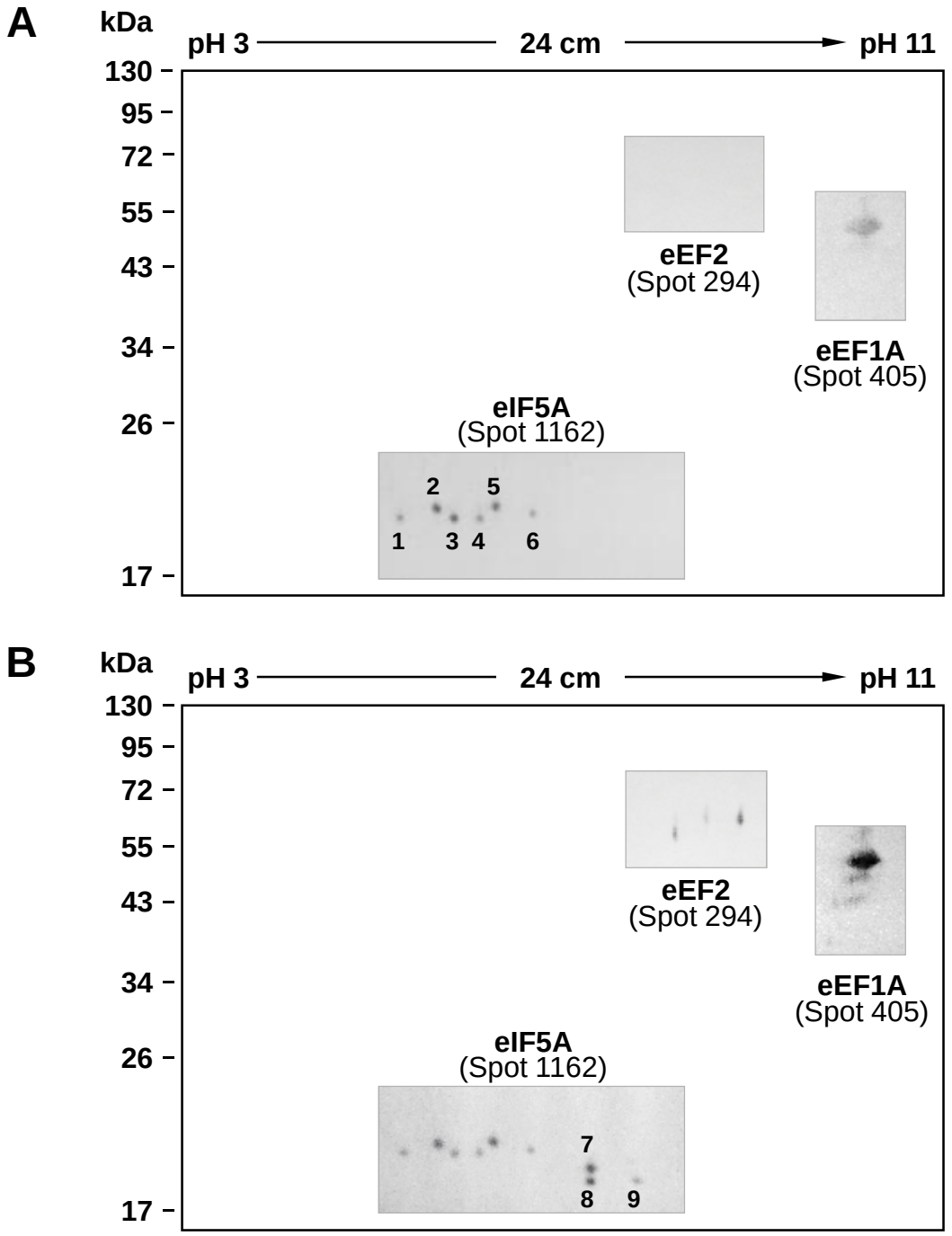
A
kDa
pH 3
24 cm
pH 11
130
95
72
55
43
34
26
17
eEF2
(Spot 294)
eEF1A
(Spot 405)
eIF5A
(Spot 1162)
1
2
3
4
5
6
B
kDa
pH 3
24 cm
pH 11
130
95
72
55
43
34
26
17
eEF2
(Spot 294)
eEF1A
(Spot 405)
eIF5A
(Spot 1162)
7
8
9

Figure 5

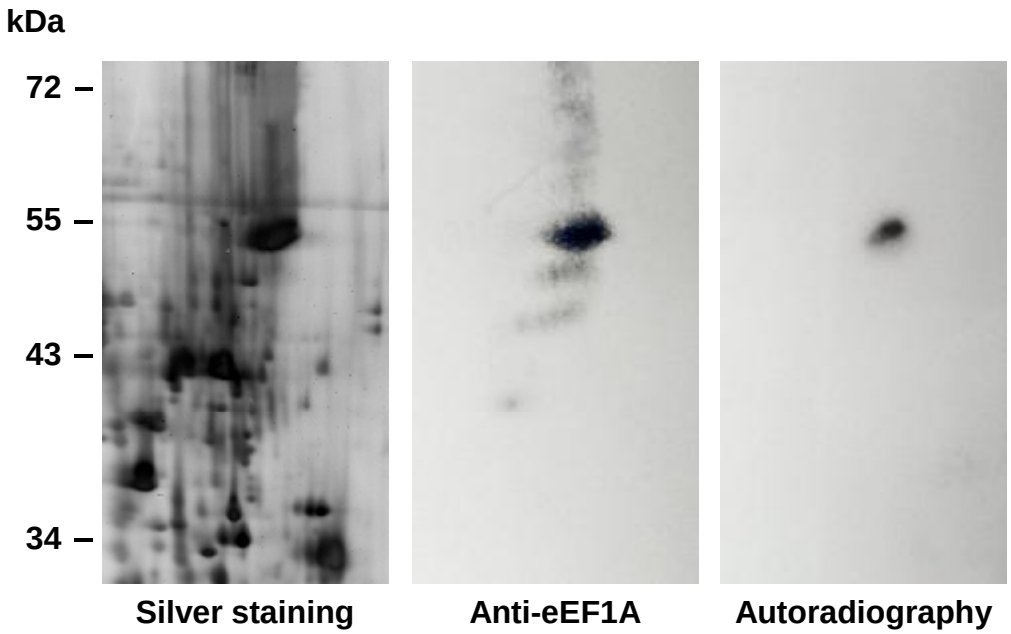

Figure S1

(Next page). Differential protein accumulation between control and CEVd-infected plants. Representative spots from Figure 1B were quantified using the DeCyder software.

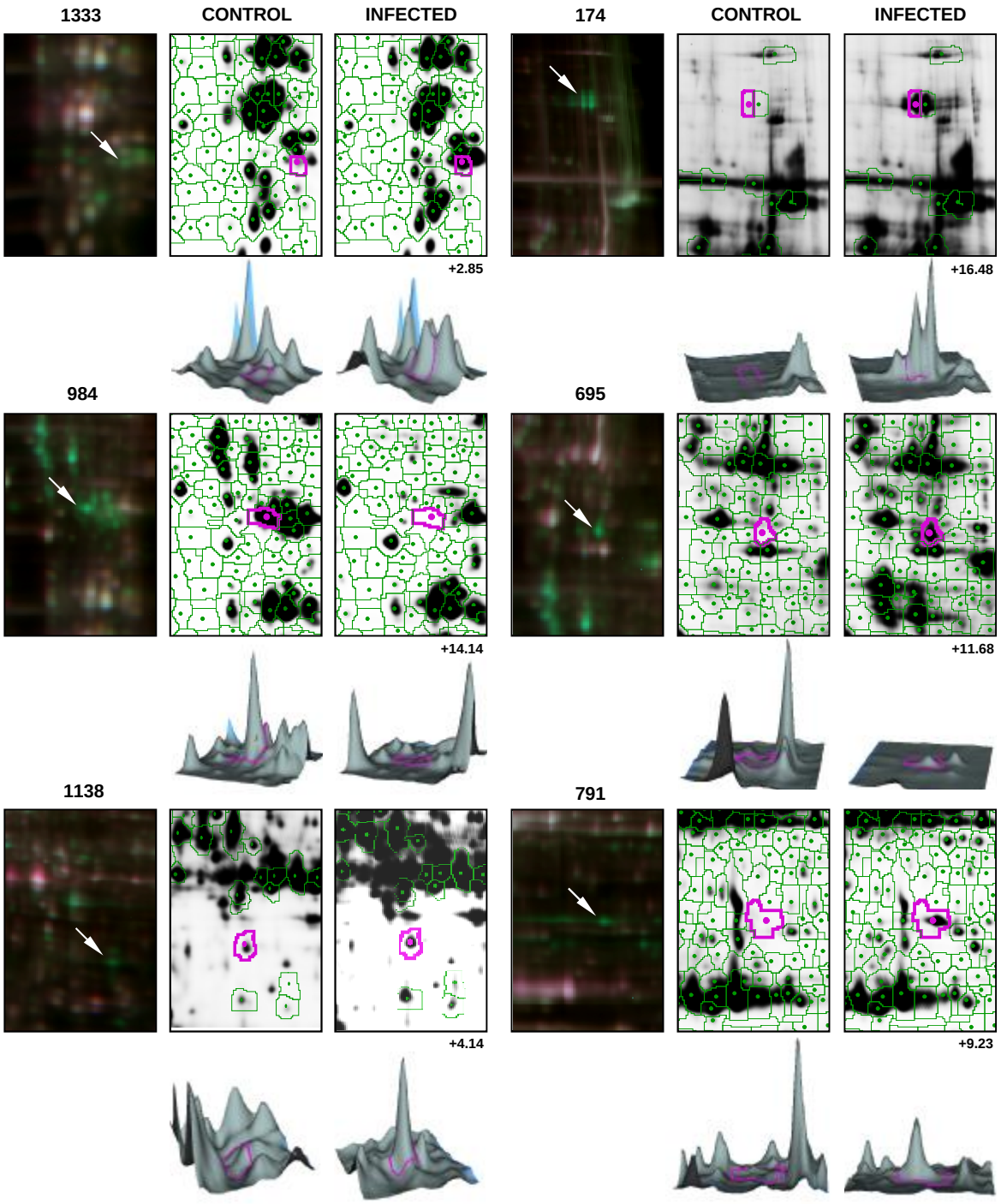
1333
CONTROL
INFECTED
+2.85
174
CONTROL
INFECTED
+16.48
984
+14.14
695
+11.68
1138
+4.14
791
+9.23

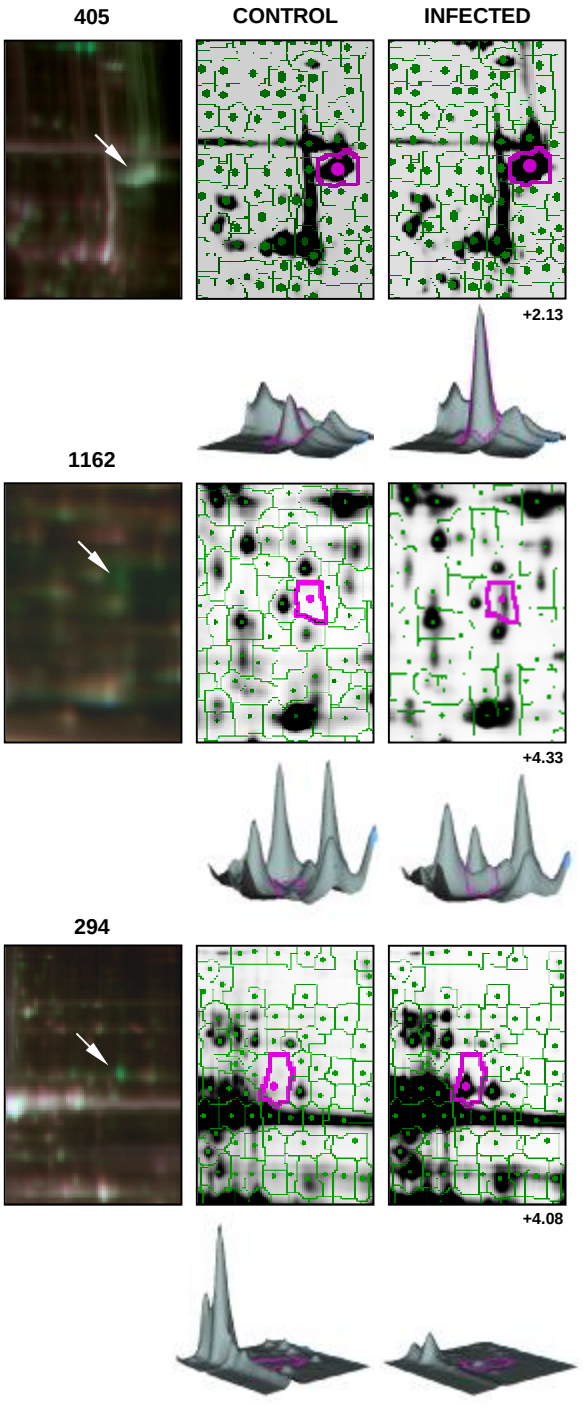
405
CONTROL
INFECTED
+2.13
1162
+4.33
294
+4.08

Figure S2A

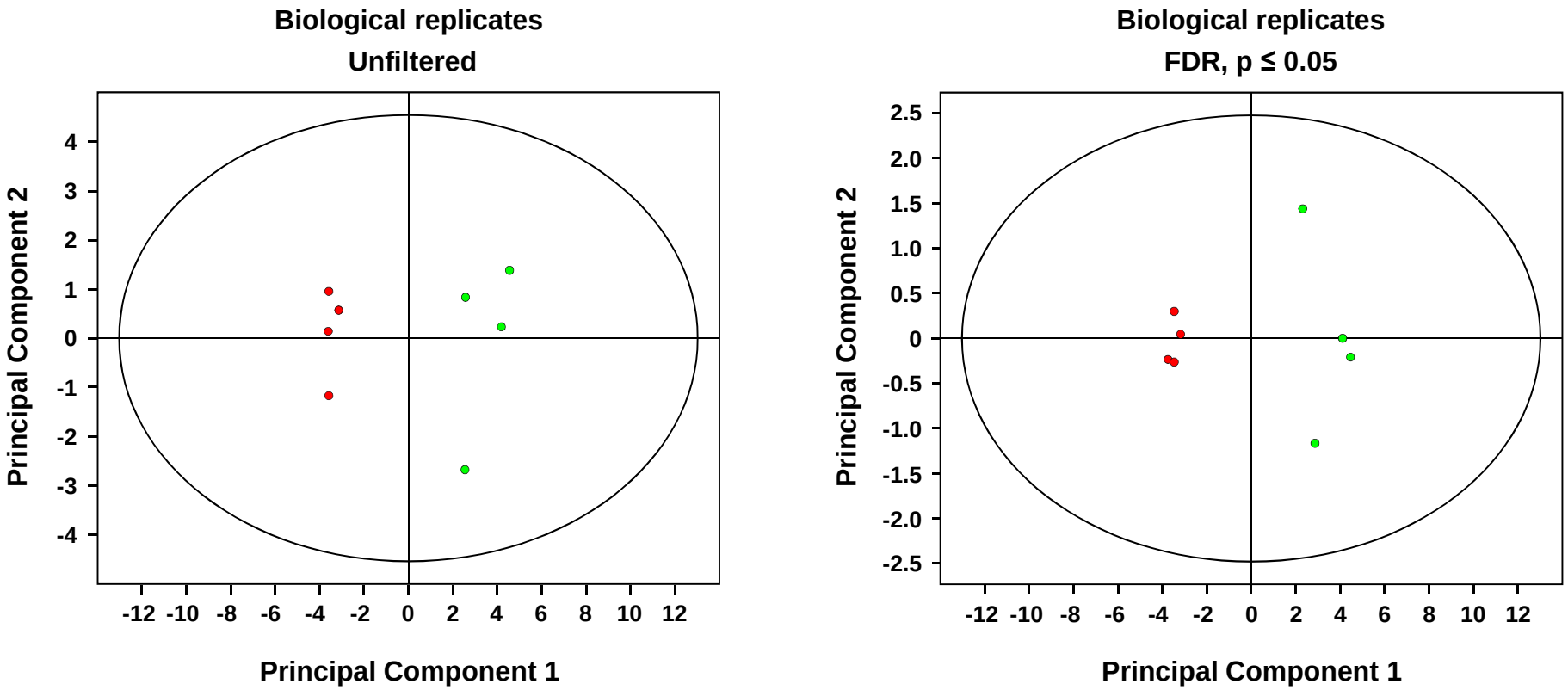

Principal component analysis (PCA) of the proteome data corresponding to four biological repeats. The proteome PCA separates healthy control plants (red) and viroid-infected plants (green). Left panel: PCA of unfiltered proteome data. Right panel: PCA of proteome data at a given FDR threshold (0.05).

Figure S2B

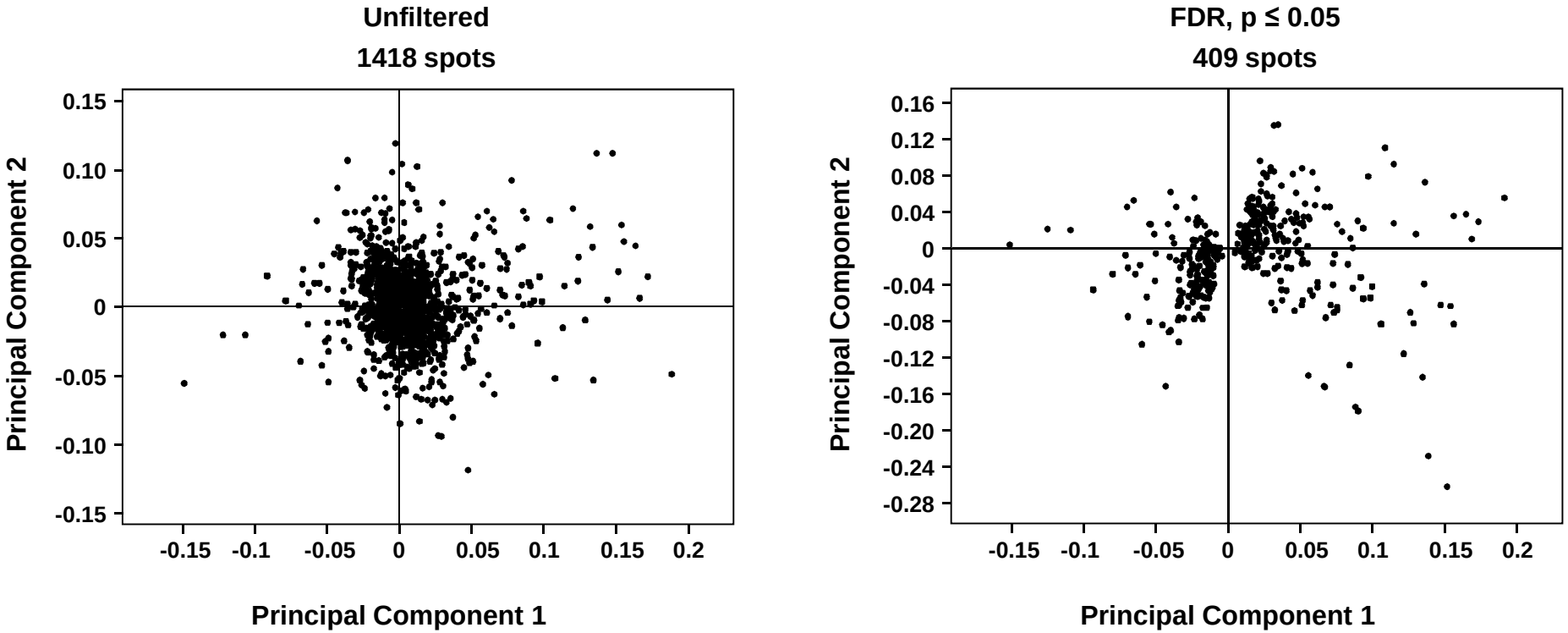

Principal component analysis (PCA) of the proteome data. Left pannel: PCA of unfiltered proteome data (1418 spots). Right pannel: PCA of proteome data at a given FDR threshold (409 spots).

Figure S3A

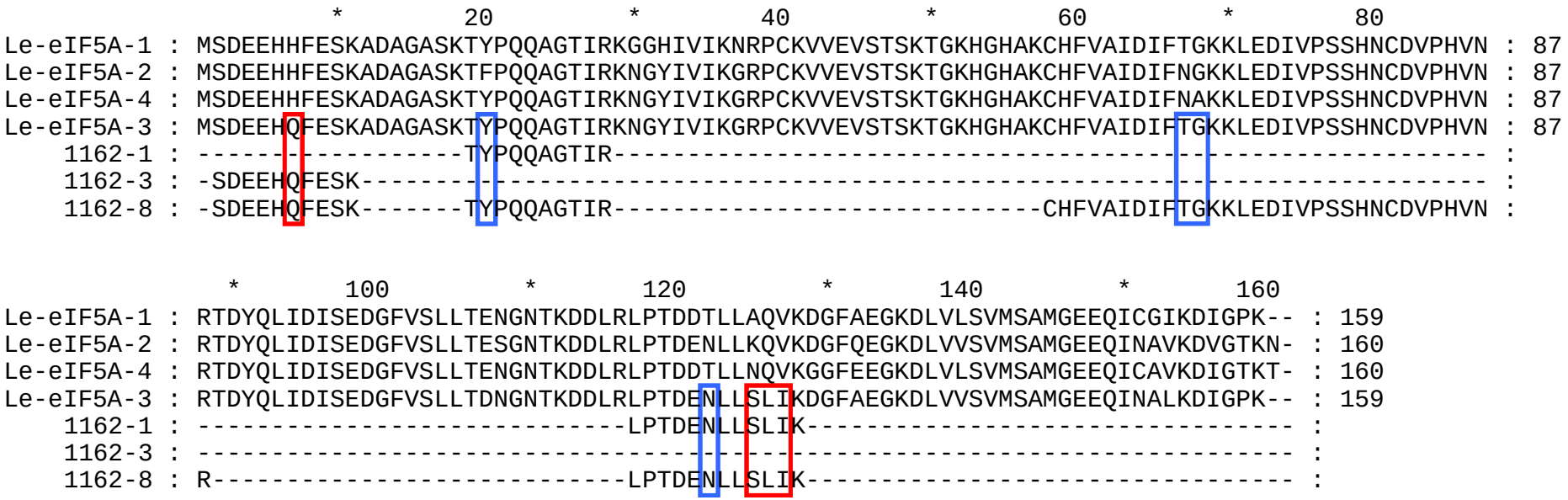

Spots 1162-1, 1162-3 and 1162-8 correspond to eIF5A-3 isoform. Peptide sequences corresponding to spots 1162-1, 1162-3 and 1162-8 were obtained by MALDI MS/MS and/or LC/MS/MS analyses, and aligned with the four tomato eIF5A isoforms. Matches indicating unambiguous correspondence to eIF5A-3 isoform are boxed in red. Other differences among isoforms which are present in the obtained peptide sequences are boxed in blue.

Figure S3B

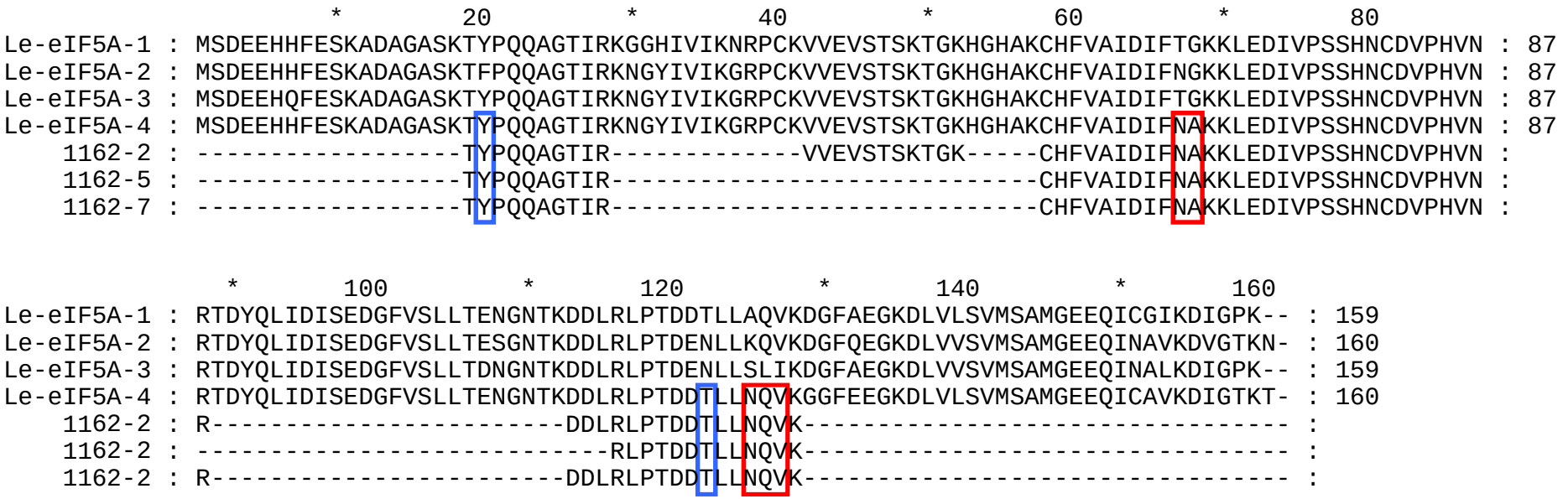

Spots 1162-2, 1162-5 and 1162-7 correspond to eIF5A-4 isoform. Peptide sequences corresponding to spots 1162-2, 1162-5 and 1162-7 were obtained by MALDI MS/MS and/or LC/MS/MS analyses, and aligned with the four tomato eIF5A isoforms. Matches indicating unambiguous correspondence to eIF5A-4 isoform are boxed in red. Other differences among isoforms which are present in the obtained peptide sequences are boxed in blue.

Figure S3C

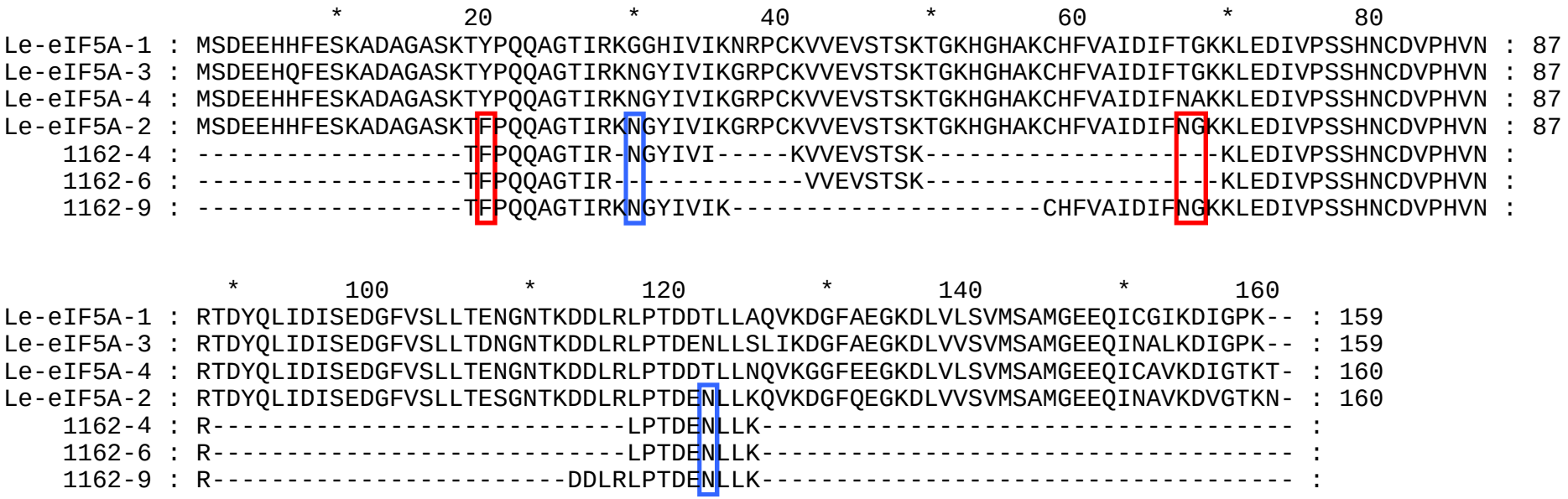

Spots 1162-4, 1162-6 and 1162-9 correspond to eIF5A-2 isoform. Peptide sequences corresponding to spots 1162-4, 1162-6 and 1162-9 were obtained by MALDI MS/MS and/or LC/MS/MS analyses, and aligned with the four tomato eIF5A isoforms. Matches indicating unambiguous correspondence to eIF5A-2 isoform are boxed in red. Other differences among isoforms which are present in the obtained peptide sequences are boxed in blue.